BREEDING VECTORS AND PREDICTABILITY IN THE OXFORD MARS GCM.

C. E. Newman, P. L. Read, S. R. Lewis, *Atmospheric, Oceanic and Planetary Physics, Department of Physics, University of Oxford, England (newmanc@atm.ox.ac.uk).*

Introduction

A breeding vectors approach is used to study the intrinsic predictability of the Martian atmosphere using the Oxford Mars General Circulation Model (MGCM). The approach, described in detail below, is first tested using a terrestrial general circulation model, the United Kingdom Meteorological Office's Unified Model (UM), and results show growing modes of instability at mid to high latitudes on spatial scales of less than ∼1,000km, in qualitative agreement with previous studies performed using terrestrial models. For the Martian atmosphere, and in the absence of radiatively active dust transport (so using a typical background dust distribution for each time of year), the technique reveals model states with approximately zero growth factors, and modes of instability on relatively large (up to ∼5,000km) spatial scales. The implications of this for the predictability of the Martian atmosphere and for the usage of ensemble forecasting methods on Mars are also discussed.

Breeding vectors and atmospheric instability

Breeding vectors [1] and singular vectors [2] are both commonly used to find dominant modes of instability in the Earth's atmosphere (e.g. to provide optimal initial perturbations for ensemble forecasting experiments, [3,4]). Both are related to Lyapunov vectors [5], which may be used to determine the predictability of dynamical systems. For a system described by $\mathbf{F}(t)$, with

$$\mathbf{F}(t+\delta t) = \mathbf{M}[\mathbf{F}(t)]$$

where $\mathbf{M}$ is the propagator of the nonlinear model, the leading normalized Lyapunov vector may be found as follows: (1) start with some arbitrary perturbation, $\delta\mathbf{F}(t)$, (2) evolve this through one timestep using the propagator of the tangent linear model $\mathbf{L}$, i.e.,

$$\delta\mathbf{F}(t+\delta t) = \mathbf{L}[\delta\mathbf{F}(t)]$$

where $\mathbf{L} = \partial\mathbf{M}/\partial\mathbf{F}$, (3) repeat (2) until $\delta\mathbf{F}$ converges (on the leading Lyapunov vector). Other Lyapunov vectors may be obtained by orthogonalizing after each time step with respect to the subspace of the previous Lyapunov vectors.

Bred vectors also begin with an arbitrary initial perturbation $\delta\mathbf{F}(t)$, but now this is added to the initial state $\mathbf{F}(t)$ and the perturbed state is evolved to time $t+\delta t$ using the full nonlinear model. The perturbation at time $t+\delta t$ is therefore given by

$$\delta\mathbf{F}(t+\delta t) = \mathbf{M}[\mathbf{F}(t)+\delta\mathbf{F}(t)] - \mathbf{M}[\mathbf{F}(t)].$$

As before, this process is repeated until there is convergence, however after each breeding time step (or 'breeding cycle') the size of $\delta\mathbf{F}(t+\delta t)$ is renormalized to that of the initial perturbation, where size is defined using some global 'norm' (discussed further below). Renormalization is necessary to prevent/control nonlinear saturation of the instabilities of interest, although an advantage of the breeding vector method is that the size of the initial perturbations may be chosen to filter out naturally any instabilities which have fast growth factors, but which saturate nonlinearly at such small amplitudes that they are irrelevant for forecasting applications. Lyapunov and singular vectors, by contrast, may be dominated by such small amplitude instabilities unless they are explicitly excluded from the tangent linear model used.

Methodology

The bred vectors are produced as follows (see e.g. [6]): a control run C is begun from a suitable initial state, then a perturbation run P is begun from the same initial state but with added random (white noise) perturbations. Run P proceeds for e.g. 6 hours, then the perturbations (represented by the differences between P and C at all locations) are renormalized so that some globally-averaged quantity (the 'norm') is restored to the same size as it was initially. For example, the rms potential vorticity 'norm' is given by $Q = \sqrt{\frac{1}{N}\sum_i^N (\Delta q)_i^2}$, where $(\Delta q)_i$ is the difference in PV at grid point i, and N is the number of points (in practise there is also mass weighting). This renormalization is repeated every 6 hours until the perturbations have formed into the fastest growing (most unstable) modes.

Applying the technique to an Earth GCM

The Met Office Unified Model was used to find breeding vectors for the Earth's atmosphere. Since this technique has not been applied Mars until now, and in the light of some slightly unexpected results for Mars, it was deemed necessary to test the method by applying it to the Earth's

atmosphere, for which there are already results available for comparison.

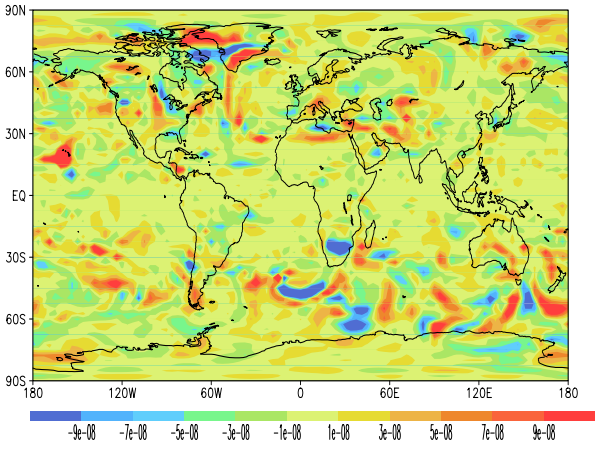

Figure 1: Potential vorticity perturbations after 10 sols of a breeding run performed during northern hemisphere winter (January) for Earth using the Unified model with a resolution of ∼2.5 degrees longitude by ∼3.75 degrees latitude.

Figure 1 shows breeding vectors (as represented by the potential vorticity perturbation) at 250hPa after 10 sols of an experiment conducted during northern hemisphere winter (January), and using mean initial white noise temperature perturbations of ∼5K. Comparable patterns are found after 2 sols at a range of other pressure levels. The greatest amplitudes are at mid to high latitudes, and certain regions of strong instability can be seen to be off the tip of Africa, most longitudes at ∼50–60 degrees south, and over northern Canada and Greenland. The pattern of instability is qualitatively similar to that found using a breeding vectors approach in other Earth general circulation models [4], or using other methods (e.g., singular vectors [5]).

Figure 2 shows growth factors for two experiments, with mean initial temperature perturbations of ∼10K (solid line) and ∼1K (dashed line). These are the factors by which the global rms potential vorticity increased during each breeding cycle (prior to renormalization). In the latter experiment, perturbations have a mean growth factor of ∼1.33 (an increase of ∼33%) per day, i.e., have to be renormalized *downwards* after each breeding cycle. Growth factors are less than 1 only during the first day, when decaying modes in the perturbation such as gravity waves are removed, requiring the remaining perturbations to be amplified at the end of the first cycle. They are also consistently greater than for the other experiment, which uses larger initial perturbations. This is because using smaller initial perturbations, and hence a smaller norm for rescaling, allows smaller amplitude, fast growing instabilities to grow without

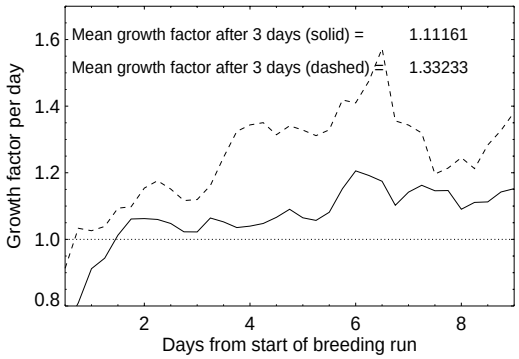

Figure 2: Perturbation growth factors for the first 10 sols of experiments similar to that in figure 1, but with initial perturbations doubled (solid line) and one fifth as large (dashed).

suffering nonlinear saturation, and so produces higher transient growth factors. Such a result is consistent with previous work [4], as is the result that the choice of 'norm' has relatively little impact – to date, rms kinetic energy and potential vorticity norms have been tested for the UM.

Applying the technique to the Oxford Mars GCM

In applying the breeding vectors method in an MGCM, care is first required in choosing, for example, suitable initial perturbation amplitudes, since there is no previous work to indicate how sensitive results may be to such choices. To investigate this, breeding runs have been performed at two model resolutions, T21 and T31 (giving resolutions better than 7.5 and 5 degrees, respectively), using initial average temperature perturbations of ∼0.2K – ∼10K, and with different dust loadings. All of these factors appear to be significant in determining the modes of instability which grow the fastest without saturating (and hence appear as bred vectors), and in particular affect the overall perturbation growth factors.

To demonstrate this, a series of experiments were conducted near northern autumn equinox (Ls∼180 degrees). For each experiment, initial white noise temperature perturbations of a given mean size were used with a streamfunction norm, and renormalization took place four times per sol. The model used was the MGCM, basically the Oxford version of the European Mars general circulation model described fully in [7], run with different prescribed dust distributions.

Figure 3 shows the structure of the bred vectors (as a streamfunction perturbation) at 80Pa after 30 sols of two

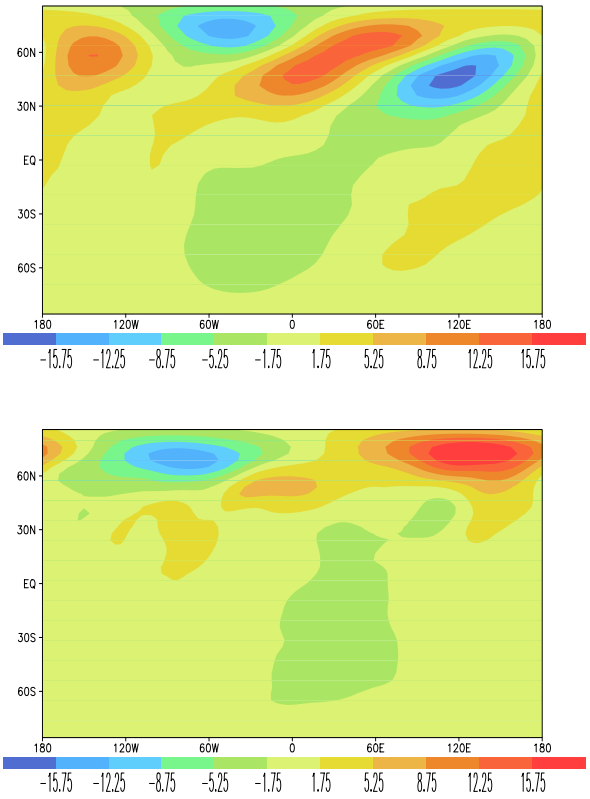

Figure 3: Streamfunction perturbations (in arbitrary units) after 30 sols of a breeding run during northern autumn on Mars (Ls∼180 degrees). The MGCM was used with the MGS dust scenario and mean temperature perturbations of ∼5K, run at T21 (top) and T31 (bottom) resolution.

simulations which used a mean temperature perturbation of ∼5K and the 'MGS dust scenario'. This dust scenario was designed to produce a good match to the first year of Mars Global Surveyor temperature observations, so the model state produced is a 'best guess' to the state on Mars over that period. The only difference between the plots is the model resolution used to produce them (T21 for the top panel and T31 for the bottom). At this particular time, 30 sols in, the fastest growing modes in the two simulations are different, with a wave two mode in the lower resolution experiment and a wave one pattern dominating in the second, although there are signs that both are a mixture of the two modes. The growth factors for the T31 run are shown in the top panel of figure 4, with a mean growth factor between 3 and 30 sols of ∼1.2, though there is tremendous variability over this period in terms of whether there is growth or decay. The mean growth factor between 3 and 30 sols for the T21 experiment is ∼1.135, so there is on average increased growth in the higher resolution experiment. This may be compared with the work of e.g. Hartmann et al. [8], using singular vectors in the ECMWF model of the Earth's atmosphere, who found linear growth factors to be approximately doubled when the model resolution was increased from T21 to T42. They comment that this increase (which is substantially greater than that reported here for the MGCM) is consistent with greater growth being associated with smaller spatial scales.

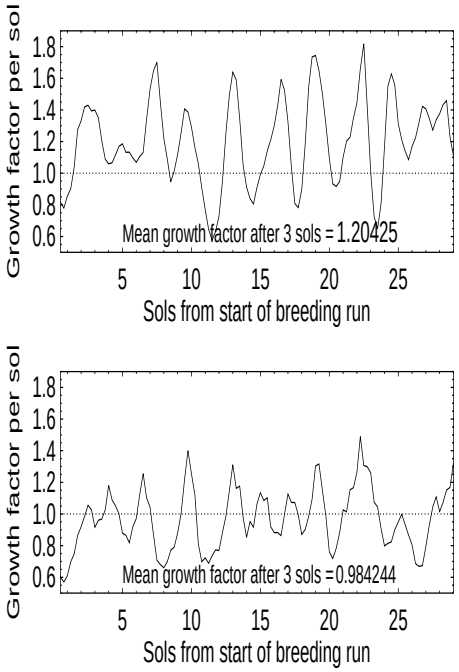

Figure 4: Perturbation growth factors for experiments at T31 resolution with mean temperature perturbations of ∼5K, using the MGS (top) and Viking (bottom) dust scenarios.

Growth factors are also increased if smaller initial perturbation amplitudes are used. For example, an MGS scenario T31 run using perturbations 10% of those in the first experiments has a mean growth factor between 3 and 30 sols of ∼1.274. This is due to the inclusion of faster growing small amplitude perturbations, which were effectively filtered out in the first runs. The bred vectors produced are similar in some respects, but also include short-lived patterns in mid and low latitudes.

The bottom panel of figure 4 shows the growth factors for a run similar to the first T31 experiment, but now using the 'Viking dust' scenario (described in [7], this has seasonally varying dust, modelled on that observed by the Viking Landers but with the large dust storms removed). The bred modes (not shown) are slightly more complex than those found in the T31 MGS run, and the mean growth factor of just under 1 indicates that there is roughly zero net growth of these modes. The lack of growth is probably due to the slightly dustier Viking scenario producing a more stable atmosphere than the

clearer MGS scenario.

Finally, figure 5 shows the bred vectors for northern hemisphere spring (Ls∼0 degrees, top panel) and summer (Ls∼90 degrees, bottom panel), using ∼5K mean perturbations at T31 resolution with the MGS dust scenario. In northern spring the modes at this level are again confined mostly to high latitudes, but are now in the spring hemisphere (as opposed to peaking in the autumn hemisphere at Ls∼180 degrees). This asymmetry is partially due to the MGS dust scenario, in which the spring hemisphere is far dustier at Ls∼180 degrees than at Ls∼0 degrees, but even using a constant dust distribution the modes tend to be more prominent in the northern hemisphere at equinox. In northern summer, however, the bred vectors are quite different. They peak in the southern (winter) hemisphere, but are now not confined to high latitudes, and have structures on far smaller spatial scales than seen in the equinoctial results.

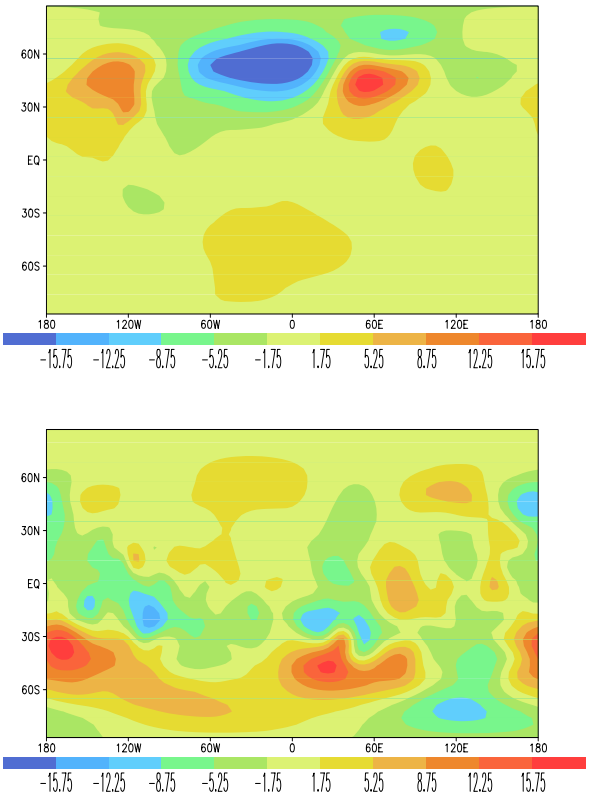

Figure 5: As in the bottom panel of Fig.3, but for northern spring (top) and summer (bottom).

Discussion

The patterns of instability in the Martian atmosphere are found to occur on far larger spatial scales than on the Earth at all times of year, and are particularly strong during equinoctial periods when large-scale baroclinic wave activity is at its peak. The modes of instability generally peak at high latitudes, and their westward tilt with height suggests that they are indeed baroclinic in origin. Growth factors are lower than on Earth for comparable perturbation magnitudes, and are highly variable rather than tending to a relatively steady value (as observed for the Earth). The tendency for modes to oscillate between growth and decay is an unexpected result, and further study is required to determine whether this is truly representative of their behaviour on Mars. Mean growth factors, however, are found to increase if the mean size of the initial perturbations is reduced (enabling growth of lower amplitude, often faster growing modes, without nonlinear saturation), and if the model resolution is increased (enabling spatially smaller effects to be included). Growth is reduced if a globally dustier, and therefore more stable, atmosphere is used.

At this preliminary stage there is still much to investigate before any ensemble forecasting experiments can be attempted, most importantly the significance of the variable growth factors and also the impact of including radiatively active dust advection. This would be expected to increase growth factors substantially via feedbacks between the circulation and dust distribution.

References

[1] Toth, Z. and E. Kalnay, *Ensemble forecasting at NCEP and the breeding method*, Monthly Weather Rev., vol.125, no.12, pp.3297-3319, 1997.

[2] Molteni, F. and T.N. Palmer, *Predictability and finite-time instability of the northern winter circulation*, Q.J. R.Meteorol.Soc., vol.199, no.510, pp.269-298, 1993.

[3] Toth, Z. and E. Kalnay, *Ensemble forecasting at NMC – the generation of perturbations*, Bull.Am.Meteorol. Soc., vol.74, no.12, pp.2317-2330, 1993.

[4] Molteni, F., R. Buizza, T.N. Palmer and T. Petroliagis, *The ECMWF ensemble prediction system: Methodology and validation*, Q.J.R.Meteorol.Soc., vol.122, no. 529, pp.73-119, 1996.

[5] Kalnay, E., M. Corazza and M. Cai, *Are bred vectors the same as Lyapunov vectors?*, INFM-DIFI, Universita di Genova, 2001.

[6] Corazza, M. et al., *Use of the breeding technique to estimate the structure of the analysis "errors of the day"*, submitted to Nonlin.Proc.Geophys., 2002.

[7] Forget, F. et al., *Improved general circulation models of the Martian atmosphere from the surface to above 80 km*, J.Geophys.Res., vol.104, E10, pp.24155-24175, 1999.

[8] Hartmann, D. L., R. Buizza and T.N. Palmer, *Singular vectors – the effect of spatial scale on linear growth of disturbances*, J.Atmos.Sci., vol.52, no.22, pp.3885-3894, 1995.